Tubulin Acetylation Enhances Microtubule Stability in Trabecular Meshwork Cells Under Mechanical Stress

Chien-Chia Su,[1,2] Vaibhav Desikan,[1] Kevin Betsch,[1] Myoung Sup Shim,[1] Kate E. Keller,[3] and Paloma B. Liton[1]

[1]Department of Ophthalmology, Duke Eye Center, Duke University, Durham, North Carolina, United States
[2]Department of Ophthalmology, National Taiwan University Hospital, Taipei, Taiwan
[3]Casey Eye Institute, Oregon Health & Science University, Portland, Oregon, United States

Correspondence: Paloma B. Liton, Department of Ophthalmology, Duke University Eye Center, Duke University, AERI Building, Office 4004, Box 3802, 2351 Erwin Rd., Durham, NC 27713, USA; paloma.liton@duke.edu.

Received: September 27, 2024
Accepted: December 29, 2024
Published: January 17, 2025

Citation: Su CC, Desikan V, Betsch K, Shim MS, Keller KE, Liton PB. Tubulin acetylation enhances microtubule stability in trabecular meshwork cells under mechanical stress. *Invest Ophthalmol Vis Sci.* 2025;66(1):43. https://doi.org/10.1167/iovs.66.1.43

Purpose. To study the roles of tubulin acetylation and cyclic mechanical stretch (CMS) in trabecular meshwork (TM) cells and their impact on outflow pathway physiology and pathology.

Methods. Primary TM cell cultures were subjected to CMS (8% elongation, 24 hours), and acetylated α-tubulin at lysine 40 (Ac-TUBA4) was assessed by western blotting and immunofluorescence. Enzymes regulating tubulin acetylation were identified via siRNA-mediated knockdowns of ATAT1, HDAC6, and SIRT2. Ac-TUBA4 levels were compared between glaucomatous (GTM) and non-glaucomatous (NTM) TM cells and in frozen sections of human cadaver eyes. The effect of tubulin acetylation on substrate stiffness and cell contractility was evaluated by culturing cells on substrates with varying stiffness and by collagen gel contraction assays, respectively. Microtubule stability was examined by monitoring resistance to nocodazole-induced depolymerization. The in vivo effect on intraocular pressure (IOP) was evaluated following intracameral injections of tubacin in mice.

Results. CMS induced tubulin acetylation in human TM cells by downregulating the deacetylase HDAC6. Elevated Ac-TUBA4 levels were observed in GTM compared NTM cells and tissues. Tubulin acetylation was not affected by substrate stiffness and did not show a direct effect on TM cell contractility. Tubulin acetylation was found to provide protection against microtubule destabilization induced by nocodazole. Importantly, intracameral injection of tubacin, an HDAC6 inhibitor, significantly lowered IOP in mice.

Conclusions. Our study highlights a critical role of tubulin acetylation in TM cell response to mechanical stress and its potential impact on IOP regulation. Tubulin acetylation could represent a therapeutic target for glaucoma.

Keywords: trabecular meshwork, glaucoma, tubulin acetylation, mechanical stress

Mechanical forces in the trabecular meshwork (TM)/Schlemm's canal (SC) conventional outflow pathway are believed to play a key role in regulating aqueous humor (AH) homeostasis and intraocular pressure (IOP).[1] Cells within the outflow pathway experience tensile or mechanical stretch due to pressure differences and fluctuations in ocular pressure caused by pulsation or activities such as blinking and saccades. Additionally, outflow pathway cells are subjected to shear stress generated from the flow of AH as it travels through the TM and SC tissues.[2]

Mechanical stretch triggers a dynamic response in the cytoskeleton, which may fluidize to accommodate the force or reinforce to resist it, depending on the magnitude and duration of the stress.[3–5] This mechanoresponse involves intricate coordination among cytoskeletal components, including microtubules, which play a pivotal role in sensing mechanical forces and stabilizing cellular structures.[6] A substantial body of research has demonstrated that both TM and SC cells can sense mechanical forces and respond by triggering various cellular processes aimed at adjusting outflow resistance, including cytoskeletal remodeling.[4,7,8] Although the effects of mechanical forces on the actin cytoskeleton and focal adhesions have been extensively studied in outflow pathway cells,[4,7,9,10] no research has yet explored the relationship between mechanical stretch and the microtubule (MT) cytoskeleton in TM and SC cells.

Microtubules are a crucial component of the cytoskeleton of a cell. They play a vital role in maintaining cell shape, enabling intracellular transport, and facilitating cell division.[11] Beyond these functions, microtubules are also essential in cell biology and are involved in the mechanical response of a cell to external forces.[12] They contribute to the ability of the cell to sense and react to mechanical stress, supporting cell rigidity and stability. Structurally, MTs are tubular formations composed of α- and β-tubulin dimers, which assemble into protofilaments. Typically, 13 protofilaments align side by side to form a hollow tube. This structure is highly dynamic, allowing microtubules to undergo rapid polymerization and depolymerization, a process known as

Investigative Ophthalmology & Visual Science

dynamic instability, which is essential for their various cellular functions.[13] The functional diversity of the MTs depends on the differential expression of tubulin isotypes and the various post-translational modifications.[11,14]

Tubulin acetylation, specifically at the lysine 40 (K40) residue of α-tubulin, is a critical post-translational modification associated with the stabilization and mechanical properties of MTs.[15–18] This modification is predominantly found on long-lived MTs, including those in cilia, flagella, centrioles, and stable cytoplasmic MTs with slow dynamics that resist depolymerization.[13,19,20] Acetylation of tubulin is catalyzed by α-tubulin *N*-acetyltransferase 1 (α-ATAT1), which transfers an acetyl group from acetyl-coenzyme A to the K40 residue,[20–22] whereas deacetylation is mediated by histone deacetylase 6 (HDAC6) and sirtuin 2 (SIRT2).[17] Tubulin acetylation enhances the flexibility and resilience of microtubules, serving a protective role against mechanical stress and preventing structural damage.[15,23,24]

In this study, we investigated the dynamic regulation and functional significance of tubulin acetylation in TM cells in response to cyclic mechanical stretch (CMS) in control and glaucomatous TM cells and the role of tubulin acetylation on IOP in vivo in mice. To our knowledge, this is the first study to explore the function of tubulin acetylation in the regulation of outflow pathway dynamics.

Materials and Methods

Reagents

Chemicals and other materials were obtained from the following sources: Dimethyl sulfoxide (DMSO; D2650), bovine serum albumin (BSA; A7906), bovine gelatin (G1393), TGFβ2 (T2815), tubacin (SML0065), and nocodazole (M1404), were all from Sigma-Aldrich (St. Louis, MO, USA). Dulbecco's Modified Eagle Medium (DMEM; 11885084), Dulbecco's Phosphate-Buffered Saline (DPBS; 14190235), 100× penicillin–streptomycin (Pen/Strep; 15240062), 100× penicillin–streptomycin–glutamine (10378016), fetal bovine serum (FBS; 10082147), non-essential amino acids (11140050), gentamicin (15750060), Lipofectamine RNAiMAX Reagent (13778075), 4′,6-diamidino-2-phenylindole (DAPI; 62248), ECL Western Blotting Substrate (32106), and SuperSignal West Femto Maximum Sensitivity Substrate (34096), were all obtained from Thermo Fisher Scientific (Waltham, MA, USA). Precision Plus Protein All Blue Prestained Protein Standards (161-0373) and polyvinylidene fluoride (PVDF) membrane for protein blotting (1620177) were obtained from Bio-Rad Laboratories (Hercules, CA, USA).

Cell Culture

Primary human TM (HTM) cells were isolated from dissected TM tissue obtained from discarded corneal rims following corneal transplantation surgeries at Duke University Eye Center and maintained as previously described.[25] Each culture originated from one or two corneal rims from the same donor, depending on availability. Cells were passaged at a 1:2 ratio upon reaching confluence, and cells from passages 4 to 8 were used for this study. Characterization of HTM cells was confirmed by their morphology and the upregulation of myocilin in response to dexamethasone treatment, in line with standard recommendations for TM cell isolation, characterization, and culture.[26] All protocols involving human tissue were approved by the Duke University Institutional Review Board (protocol #00050810) and followed the tenets of the Declaration of Helsinki. Non-glaucomatous (NTM) and glaucomatous (GTM) cells were obtained from the laboratory of Kate Keller, PhD. These cells were cultured from TM tissue dissected from human cadaver eyes, provided by VisionGift (Portland, OR, USA), following established procedures.[26] Donor information was deidentified prior to use. The use of cadaver eyes was considered exempt by the Oregon Health & Science University Institutional Review Board. Donor demographics are detailed in Supplementary Table S1. When indicated, cells were grown on 5-kPa and 60-kPa CellSoft BioFlex culture plates (Flexcell International, Burlington, NC, USA), mimicking the estimated stiffness in normal and glaucomatous TM tissues.

Human Tissue

Human eyes were obtained within 24 hours postmortem from the Duke BioSight Tissue Repository. Tissues from eye donors were manipulated at all times in accordance with the tenets of the Declaration of Helsinki. Donor demographics are detailed in Supplementary Table S2.

Mechanical Stretch

CMS was applied using the Flexcell FX-5000 Tension System (Flexcell International), as described previously.[27] Briefly, cells were plated on flexible silicone-bottom plates coated with type IV collagen (Flexcell International) and grown to confluency. Mechanical stretch (8% elongation, 1 cycle/second) was then applied for 24 hours. Control cells were cultured under identical conditions but without the application of mechanical force.

siRNA Transfection

Primary HTM cells plated on 24-well plates at 80% confluence were transfected with 5 pmol of siRNA against SIRT2 (siSIRT2, sc-40988), HDAC6 (siHDAC6, sc-35544), or ATAT1 (siATAT1, sc-95272) using Lipofectamin RNAiMAX Reagent, according to the manufacturer's instructions. Cells transfected with a non-targeting siRNA (siCNT, sc-37007, 5 pmol) were used as control. All siRNAs were obtained from Santa Cruz Biotechnology (Dallas, TX, USA).

Whole-Cell Tissue Lysate Preparation

Cells were washed twice in PBS, harvested, and lysed for 30 minutes in radioimmunoprecipitation assay (RIPA) buffer (R0278; Thermo Fisher Scientific) containing 1:100 Halt protease and phosphatase inhibitor cocktail (78842; Thermo Fisher Scientific). Lysates were subjected to three cycles of thawing and freezing and were clarified by centrifugation. Protein concentration was quantified by Bradford assay using a protein assay dye reagent (5000006; Bio-Rad Laboratories).

Traditional Western Blot

Proteins (2.5–5 µg) were separated by sodium dodecyl sulfate–polyacrylamide gel electrophoresis (SDS-PAGE; 10%) and transferred to PVDF membranes. Membranes were blocked with 5% non-fat dry milk in phosphate-buffered

Investigative Ophthalmology & Visual Science

saline with Tween 20 (PBST; 0.1% Tween 20) for 1 hour at room temperature and incubated with primary antibodies diluted in blocking buffer overnight at 4°C. Membranes were then washed three times with PBST and incubated with peroxidase-conjugated secondary antibodies for 1 to 2 hours at room temperature. Signal was detected by using an enhanced chemiluminescence substrate system. Blots were scanned and quantified using the ChemiDoc Imaging System with Image Lab Touch software (Bio-Rad Laboratories). Actin-beta (ACTB) was used for normalization. Primary antibodies and dilutions used in the study were: anti-Ac-TUBA4 (T7451, 1:5000; Sigma-Aldrich), anti-TUBA4 (T5168, 1:5000; Sigma-Aldrich), anti-ACTB (SC-69879, 1:1000; Santa Cruz Biotechnology), anti-SIRT2 (12650S, 1:2000; Cell Signaling Technology, Danvers, MA, USA), and anti-HDAC6 (7558S, 1:2000; Cell Signaling Technology).

Automated Simple Western Blot

Samples were analyzed using automated western immunoblotting with the ProteinSimple Jess Simple Western System (Bio-Techne, San Jose, CA, USA); a 12- to 230-kDa module (SM-FL004) was employed for all proteins. Briefly, cell lysates were diluted to 0.5 µg/µL in 0.1× sample buffer, supplemented with 1× fluorescent molecular mass markers and 40-mM dithiothreitol (DTT), to prepare a 5-µL reaction (2.5 µg protein per reaction). The samples were heated at 95°C for 5 minutes and loaded into JESS pre-filled plates, alongside with blocking reagent, primary antibodies (Ac-TUBA4, 1:100; HDAC6, 1:50; and SIRT2, 1:50), horseradish peroxidase (HRP)-conjugated secondary antibodies (anti-mouse IgG or anti-rabbit IgG), luminol–peroxide mix, and washing buffer. After the automatic run, the digital images of chemiluminescence from the capillaries were captured using Compass for SW 6.3.0 software (Bio-Techne). The results were visualized as electropherograms, representing the peaks of chemiluminescence intensity, and as lane views, showing the chemiluminescence signals detected in the capillaries. A Total Protein Assay, using the Bio-Techne Total Protein Detection Module (DM-TP01) and Replex Module (RP-001), was included in each run for quantitation of protein loading. Quantification was performed by normalizing the areas under the protein peaks to the total protein detected. Images of the total protein assays used for normalization are included in the Supplementary Material (Supplementary Fig. S4).

Total RNA Isolation and Quantitative Real-Time PCR Analysis

Total RNA from HTM primary cultures was isolated using the RNeasy Kit (QIAGEN, Hilden, Germany), following the manufacturer's protocol, and then treated with DNase I. RNA yields and quality were determined using a DS-11 FX+ Spectrophotometer (DeNovix, Wilmington, DE, USA). First-strand cDNA was synthesized from total RNA (0.5–1 µg) by reverse transcription using Invitrogen Oligo(dT) Primer and Superscript II Reverse Transcriptase (Thermo Fisher Scientific), according to the manufacturer's instructions. Quantitative real-time PCR analysis was performed using SsoFast EvaGreen Supermix in the Bio-Rad CFX 96 system (Bio-Rad Laboratories). The following PCR parameters were used: 95°C for 5 minutes, followed by 40 cycles of 95°C for 5 seconds, 55°C for 5 seconds, and 72°C for 5 seconds. The fluorescence threshold value (C_t) was calculated by using the CFX 96 system software, and the differential mRNA expression of each gene among samples was calculated using the comparative C_t method. The absence of nonspecific products was confirmed by both analysis of the melt curves and electrophoresis in 3% Super Acryl Agarose gels. The average C_t values of the housekeeping genes β2-microglobulin (*B2M*) and β-actin mRNA were used for normalization. The sequences of the primers used for the amplifications were *ATAT-1* (F: ACCACTTTGCATCCTGGACT, R: GGTTCGGTCAATTGCCAGTTG), *B2M* (F: AGGCTATCCAGCGTACTCCA, R: TCAATGTCGGATGGATGAA), and β-actin (F: TCCCTGGAGAAGAGCTACGA, R: AGGAAGGAAGGCTGGAAGAG).

Contractility Assays

Contractility assays were conducted using the Cell Contraction Assay (CBA-201; Cell BioLabs, San Diego, CA, USA), following the manufacturer's instructions. Briefly, cells were mixed with the collagen solution at a 1:4 cell-to-collagen ratio, plated onto 24-well plates (0.5 mL per well), and incubated for 1 hour to solidify. Afterward, 1 mL of culture media was added on top of each cell–collagen matrix. Cells were allowed to grow for 1 day prior to experimental treatment. Before releasing the cell–collagen matrices with a spatula, images were captured, and the size of the matrices was recorded at indicated time points. In the experiments involving assessing the role of ATAT1 in collagen contraction, cell–collagen matrices were prepared with HTM cells transfected with siATAT1 or siCNT at 24 hours post-transfection.

Immunocytochemistry

Cells were grown on gelatin-coated 12-mm coverslips. Following treatment, cells were washed with 1× PBS containing 1 µM of nocodazole and fixed in 4% paraformaldehyde (PFA) for 30 min at room temperature. Cells were then incubated in a blocking solution of 1% goat serum and 0.1% Triton-X in PBS for 30 minutes, followed by overnight incubation at 4°C with anti-acetylated tubulin antibody (T7451, 1:3000; Sigma-Aldrich). After cells were washed with PBS, they were incubated with Alexa Fluor 488 anti-mouse antibody (1:1000) for 2 hours at room temperature. Nuclei were counterstained with DAPI and mounted. Images were acquired using an Eclipse TE2000 confocal microscope (Nikon, Tokyo, Japan) under consistent settings to ensure experimental uniformity.

Animal Husbandry

C57BL/6j mice were purchased from The Jackson Laboratory (Bar Harbor, ME, USA), and they were maintained under a 12-hour light/dark cycle, fed a standard mouse diet, and provided with water ad libitum. Animal euthanasia was performed via isoflurane asphyxiation, followed by decapitation, prior to immediate enucleation Enucleated eyes were perfused with 4% PFA for immunofluorescence. All procedures were reviewed and approved by the Institutional Animal Care and Use Committee of Duke University (Protocol Number A167-21-08) and were performed in accordance with the ARVO Statement for the Use of Animals in Ophthalmic and Vision Research and the National Institutes of Health Guide for the Care and Use of Laboratory Animals.

Investigative Ophthalmology & Visual Science

IOP Measurements

Diurnal IOP in untreated and treated eyes was measured in isoflurane-anesthetized mice using a TONOLAB rebound tonometer (iCare, Vantaa, Finland). Six measurements, taken within 5 minutes after anesthesia, were collected per eye and averaged to obtain a single IOP value per eye for each session. IOP was measured at the same time of the day to avoid circadian variations.

Tubacin Injections

A 10-µM solution of tubacin and a vehicle control were prepared and sterilized using a 0.22-µm filter. Tubacin or the vehicle control was administered to isoflurane-anesthetized C57BL/6J mice (3–4 months old; male and female; $n = 5$) via intracameral injection using a 34-gauge needle attached to a Hamilton glass syringe. All injections were performed under direct visualization through an ophthalmic surgical microscope. The needle was inserted bevel-up through the peripheral clear cornea. A small amount of AH was expressed by gently pressing on the posterior lip of the wound to allow for the injection volume. Subsequently, 2 µL of either the tubacin or vehicle solution (DMSO) was slowly manually injected. A Weck-Cel Eye Spear (Beaver-Visitec International, Waltham, MA, USA) was used to tamponade the needle tract as it was withdrawn from the anterior chamber. Cold proparacaine drops were then applied to the cornea to induce convection currents in the anterior chamber, promoting further aqueous admixture. One eye received 2 µL of tubacin, and the contralateral eye received 2 µL of the vehicle control. Additionally, daily topical instillations (one drop) of 10-µM tubacin solution or vehicle (DMSO) were applied to the respective eyes.

Immunofluorescence in Frozen Tissues

Tissue samples were fixed in 4% PFA for 24 hours and subsequently transferred to a 1% PFA solution for long-term storage. Prior to embedding, tissue samples were subjected to an increasing sucrose gradient (10%, 20%, 30% sucrose in 1× PBS) and embedded in optimal cutting temperature (OCT) compound (Tissue-Tek, Torrance, CA, USA), then rapidly frozen in dry ice. Embedded tissue was sectioned on a cryostat (10-µm thickness section), collected on charged slides (1255015; Thermo Fisher Scientific), and stored at −80°C until staining. Before immunostaining, slides were thawed at 42°C for 10 minutes and washed in 1× PBS to remove excess OCT compound. Tissue sections were permeabilized with 0.3% Triton-X/PBS for 10 minutes at room temperature and incubated in 5% BSA, 5% normal goat serum, and 0.3% Triton-X/PBS for 30 minutes at room temperature to block non-specific sites. Samples were then incubated overnight at 4°C with anti-acetylated tubulin (T7451, 1:1000; Sigma-Aldrich) and anti-CD31 (MAB13982, 1:200; Jackson ImmunoResearch Laboratories, WestGrove, PA, USA) diluted in a blocking solution, washed with 0.3% Triton-X/PBS, and incubated for 1 hour at room temperature in Invitrogen Alexa Fluor 499 or Alexa Fluor 594 goat anti-mouse antibody diluted 1:1000 in blocking solution. Nuclei were counterstained with DAPI (1:1000 in PBS), mounted in aqueous mounting media (VectaMount AQ Mounting Medium; Vector Laboratories, Newark, CA, USA), and coverslipped. Images were acquired using the Nikon Eclipse TE2000 confocal microscope under consistent laser settings to minimize variability across samples.

Statistical Analyses

For in vitro experiments, all experimental procedures were repeated at least three times in independent experiments using different HTM primary cultures. In the text and figure captions, "n" represents biological replicates with independent cell strains. For in vivo experiments, an $n = 5$ for each experimental group was used. Data are presented as the mean ± SD. Statistical analysis was carried out using Prism software (GraphPad, Boston, MA, USA) using Student's t-test between samples or, one- or two-way ANOVA with Tukey's post hoc test among groups. $P < 0.05$ was considered to be statistically significant.

Results

Cyclic Mechanical Stretch Induces Tubulin Acetylation in TM Cells

We investigated the occurrence of α-tubulin acetylation at lysine 40 (Ac-TUBA4) in HTM primary cultures with and without CMS (8% elongation) for 24 hours, using western blot and immunofluorescence analysis. Western blot in whole cell lysates showed constitutive basal levels of Ac-TUBA4 in TM cells (Fig. 1A). Ac-TUBA4 levels were significantly higher (210.9% ± 32.83%, $P < 0.0001$, $n = 8$) in stretched cultures compared to non-stretched controls. Increased Ac-TUBA4 with CMS was confirmed by immunofluorescence (Figs. 1B, 1C). A change in cellular localization was also observed. Ac-TUBA4 was predominantly localized in the perinuclear region in non-stretched cells and showed more extensive cytoplasmic staining in stretched cells. Note that, for these experiments, cells were seeded at a lower density to facilitate imaging.

HDAC6 and ATAT1 Regulate Tubulin Acetylation in TM Cells

We investigated the enzymes responsible for regulating tubulin acetylation in TM cells. For this, we knocked down ATAT1, HDAC6, and SIRT2 using specific siRNAs. The levels of Ac-TUBA4, SIRT2, and HDAC6 were assessed by western blot (Fig. 2A). Densitometric analyses confirming knockdown efficacy are included in Supplementary Figure S1. Due to the lack of a reliable commercial antibody, transcriptional downregulation of ATAT1 was confirmed by quantitative PCR instead (0.355 ± 0.101 fold, $P < 0.0001$, $n = 4$) (Fig. 2B). Knockdown of ATAT1 led to a significant decrease in Ac-TUBA4 levels compared to control cells (39.750% ± 14.68%, $P = 0.0002$, $n = 4$), as shown in Figure 2A. Conversely, knockdown of HDAC6 resulted in increased Ac-TUBA4 levels (186.5% ± 40.43%, $P = 0.005$, $n = 4$), whereas knockdown of SIRT2 had no significant effect. Together, these results indicate that ATAT1 and HDAC6 regulate tubulin acetylation and deacetylation, respectively, in TM cells.

Next, we examined whether the expression of these enzymes is altered under CMS conditions. As seen in Figure 2C, CMS significantly decreased HDAC6 protein levels (60.2% ± 22.5%, $P = 0.004$, $n = 5$) when compared to non-stretched cultures. SIRT2 levels showed a slight decrease, but it did not reach statistical significance. No changes in ATAT1 mRNA levels with CMS were observed

Investigative Ophthalmology & Visual Science

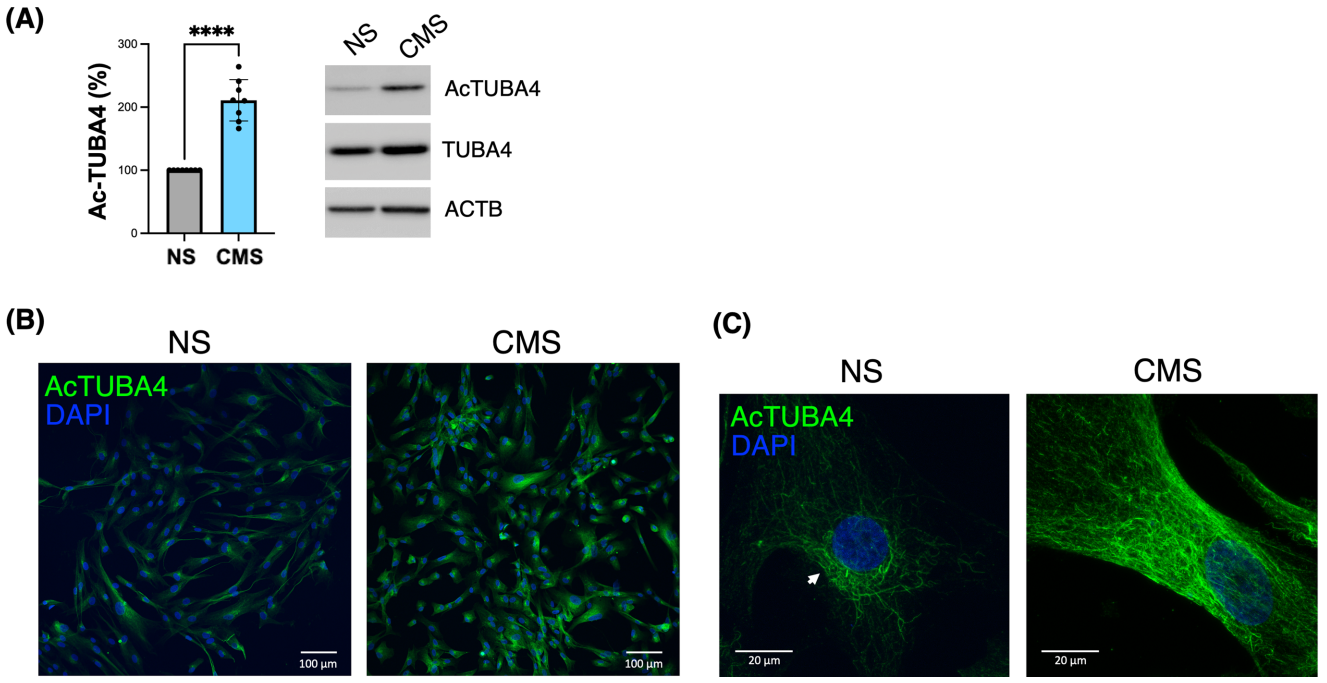

Figure 1. Tubulin acetylation in TM cells under CMS. TM primary cultures were subjected to CMS (8% elongation) for 24 hours. (**A**) Ac-TUBA4 levels evaluated by WB in whole-cell lysates ($n = 8$; $^{****}P < 0.0001$, *t*-test). (**B**, **C**) Immunocytochemical analysis at lower (**B**) and higher (**C**) magnifications. The *arrow* indicates perinuclear localization of acetylated tubulin. WB, western blot.

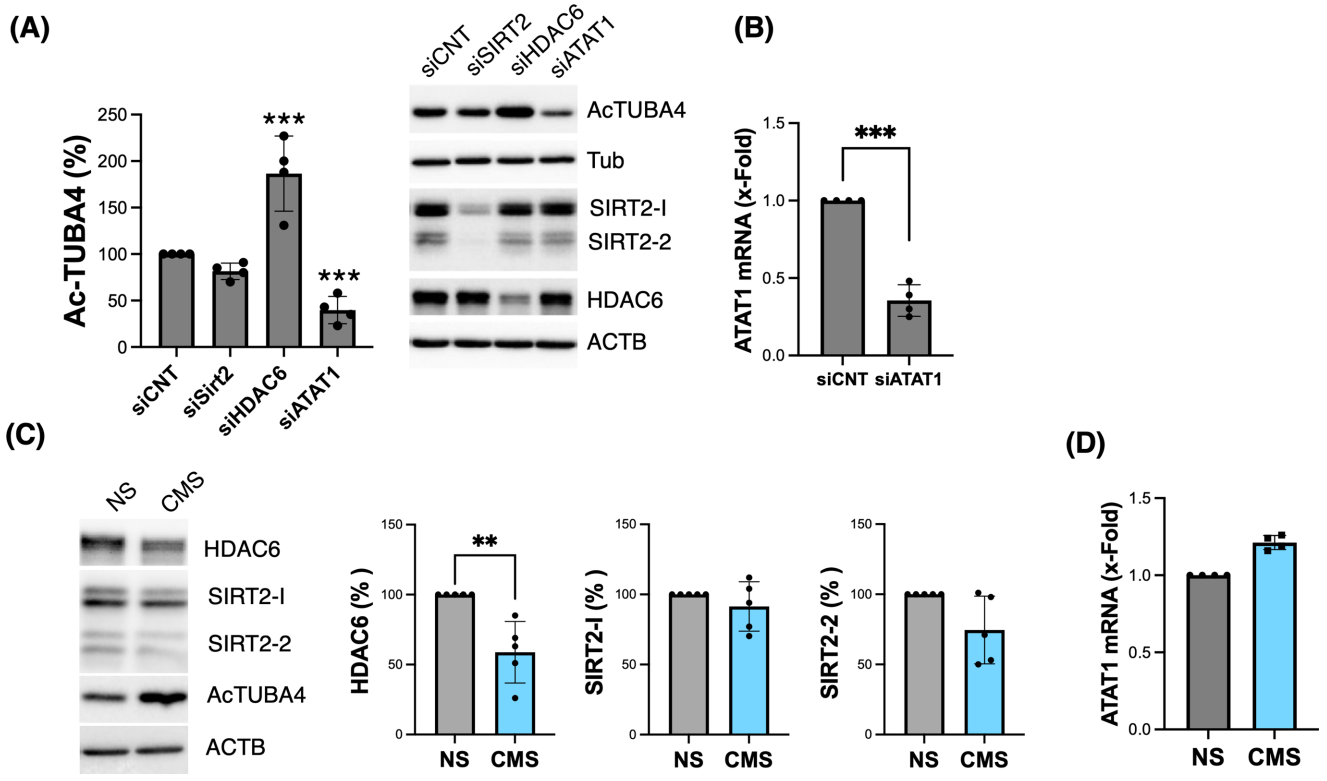

Figure 2. Identification of enzymes regulating tubulin acetylation in TM cells. (**A**) Primary TM cells were transfected with siRNAs targeting the expression of SIRT2, HDAC6, and ATAT1; siCNT was used as control. SIRT2 and HDAC6 knockdown efficiency and Ac-TUBA4 levels were evaluated at day 3 post-transfection by WB. (**B**) ATAT1 knockdown efficiency was evaluated by quantitative PCR ($n = 4$; $^{***}P < 0.001$, *t*-test). (**C**) WB quantification of HDAC6 and SIRT2 protein levels in TM cells subjected to CMS (8% elongation for 24 hours) compared to non-stretched (NS) ($n = 5$; $^{**}P < 0.01$, *t*-test). (**D**) ATAT1 mRNA quantification fold levels in TM cells subjected to CMS (8% elongation for 24 hours) compared to NS.

Investigative Ophthalmology & Visual Science

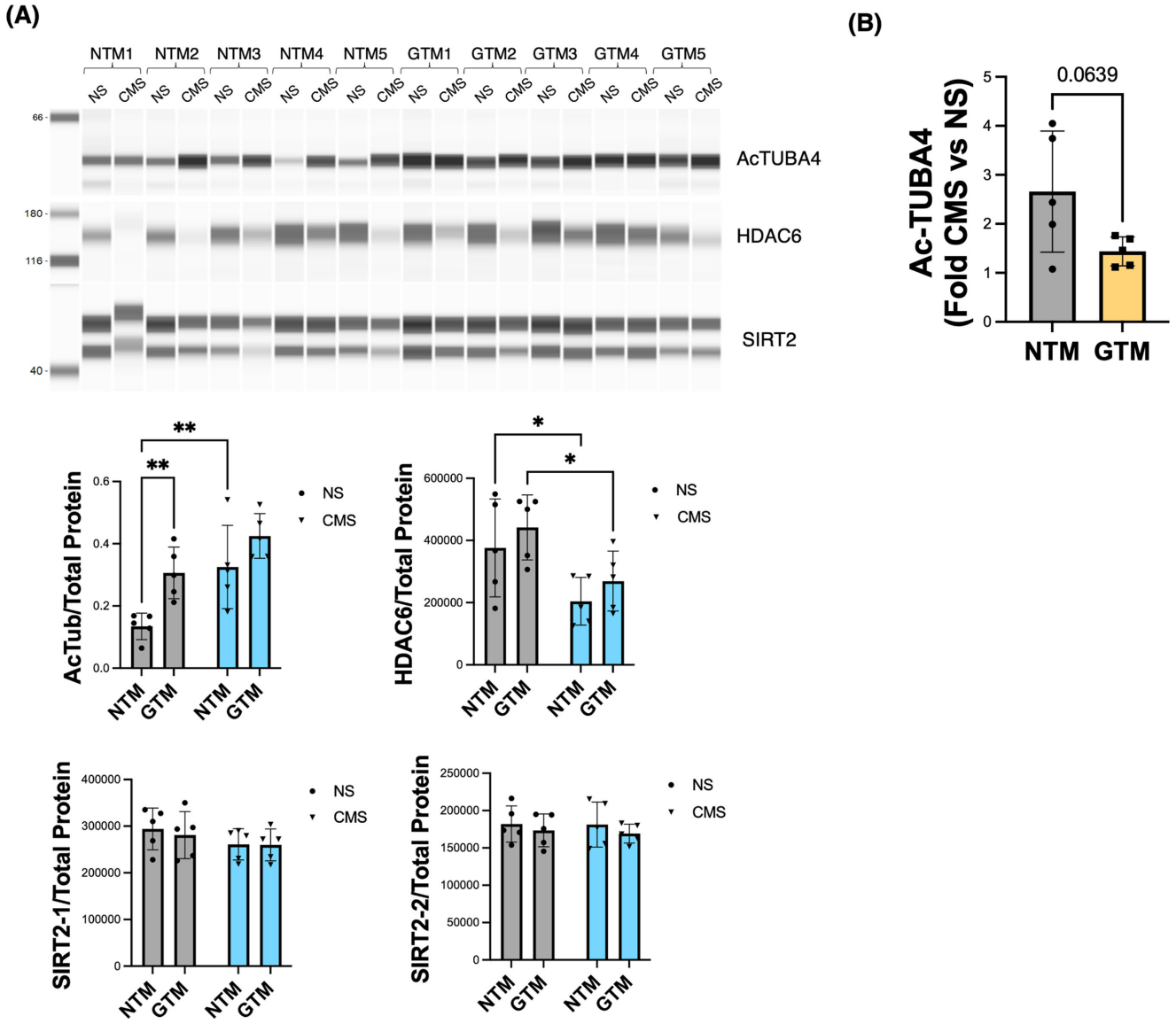

Figure 3. Tubulin acetylation in glaucomatous TM cells under non-stretched conditions and CMS. (**A**) Primary TM cells from control (NTM) and glaucomatous (GTM) cells were subjected to CMS (*blue bars*; 8% elongation for 24 hours). Protein levels of Ac-TUBA4, HDAC6, and SIRT2 were evaluated using the Jess Simple WB system and quantified using the automated built-in total protein normalization. (**B**) Fold change of Ac-TUBA4 in stretched cells compared to NS ($n = 5$; $^{*}P < 0.05$, $^{**}P < 0.01$, two-way ANOVA with multiple comparisons).

(Fig. 2D). These findings suggest that CMS increases Ac-TUBA4 by downregulating HDAC6, thereby reducing the rate of tubulin deacetylation.

Tubulin Acetylation Levels Are Elevated in Glaucomatous TM Cells

We repeated the above experiments using primary cultures of TM cells isolated from donor cadaver eyes affected by glaucoma (GTM) and age-matched controls (NTM). Notably, GTM cultures exhibited higher levels of Ac-TUBA4 compared to NTM cultures (0.306 ± 0.083 vs. 0.134 ± 0.043, $P = 0.007$, $n = 5$) in non-stretched conditions (Fig. 3A). However, no significant differences in the expression of HDAC6 or any of the SIRT2 isoforms were observed between GTM cells and NTM cells (Fig. 3A). Application of CMS further increased Ac-TUBA4 in GTM cells, although the fold induction was slightly lower than that observed in NTM cells (1.44 ± 0.3 vs. 2.65 ± 1.2 fold, $P = 0.06$) (Fig. 3B). Similar decreases in HDAC6 protein levels with CMS in NTM and GTM were noted. Images of the total protein assay used for normalization using the ProteinSimple Jess Simple Western System are included in Supplementary Figure S4 and detailed in Materials and Methods.

We investigated the presence of tubulin acetylation in situ within the outflow pathway cells by performing immunofluorescence on cryosections from control and glaucomatous human cadaver eyes. Positive Ac-TUBA4 signal was localized in the TM, particularly in the corneoscleral and uveal meshworks, with more intense staining observed near the scleral spur and ciliary muscle. No Ac-TUBA4 was detected in SC cells. Although the intensity of staining varied among

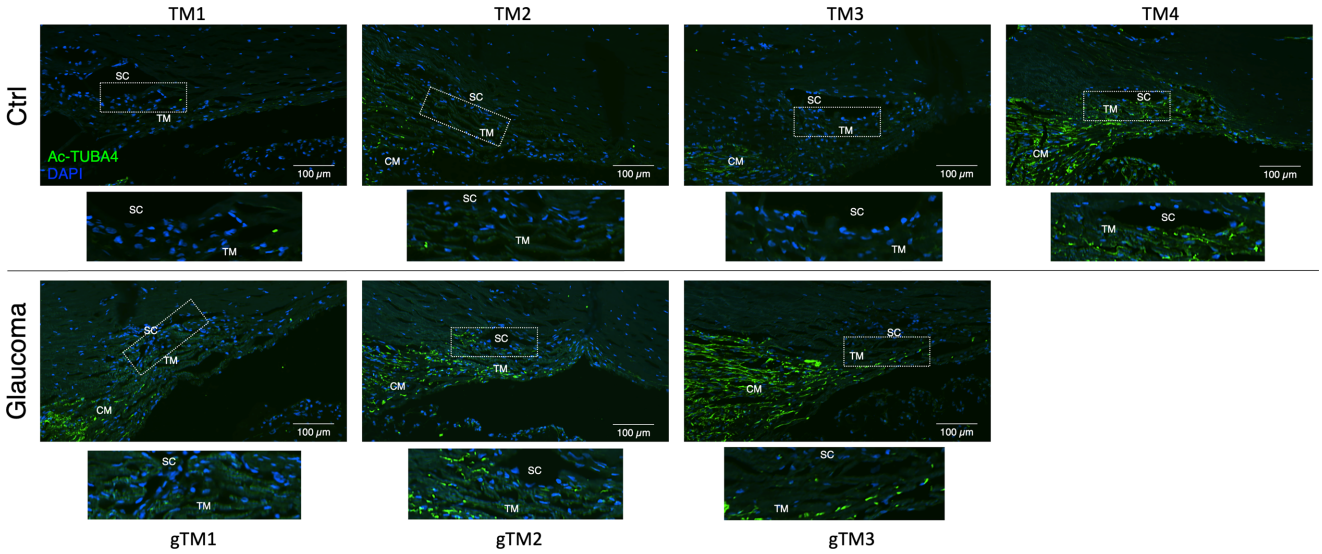

Figure 4. Immunohistological evaluation of tubulin acetylation in the outflow pathway in frozen sections from control ($n = 4$) and glaucoma ($n = 3$) human donor cadaver eyes. CM, ciliary muscle; SC, Schlemm's canal; TM, trabecular meshwork.

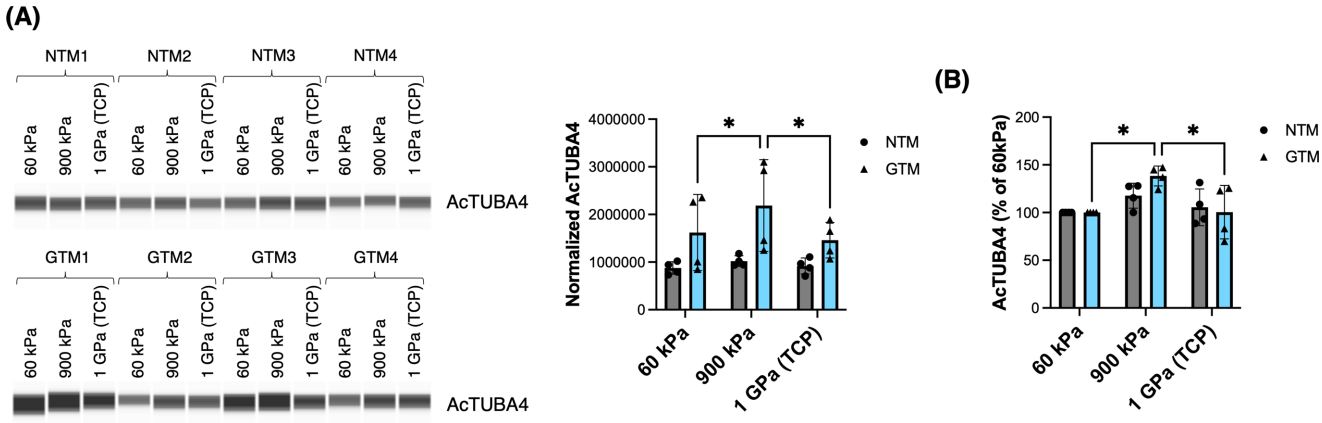

Figure 5. Effect of substrate stiffness on tubulin acetylation. Primary TM cells from control (NTM) and glaucomatous (GTM) cells were grown on 60-kPa CellSoft BioFlex culture plates, 900-kPa Flexcell plates, or plastic culture plates (~1 GPa) until confluency. (**A**) Ac-TUBA4 levels evaluated by the Jess Simple WB system and quantified using the automated built-in total protein normalization. (**B**) Percentage of Ac-TUBA4 levels for 900 kPa and TCP compared to 60 kPa ($n = 4$; $^*P < 0.05$, two-way ANOVA with multiple comparisons).

the tissues, an overall increase in Ac-TUBA4 signal was qualitatively observed in GTM eyes (Fig. 4).

Substrate Stiffness Does Not Influence Tubulin Acetylation in TM Cells

Mounting evidence suggests that the TM from glaucomatous eyes is stiffer compared with that from age-matched control eyes.[28–31] We tested whether higher Ac-TUBA4 levels in GTM cells could result from increased stiffness. For this, we measured Ac-TUBA4 levels in cell lysates from NTM and GTM cells cultured on substrates with varying stiffness: 5-kPa and 60-kPa CellSoft BioFlex culture plates, 900-kPa Flexcell plates, and tissue culture plastic plates (TCPs, ~1 GPa). Despite multiple attempts, none of the cultures was able to adapt to the 5-kPa soft condition, which approximates the physiological stiffness of non-glaucomatous TM. GTM cells consistently exhibited higher Ac-TUBA4 content compared to NTM cells, regardless of substrate stiffness (Fig. 5A). No effect of substrate stiffness on Ac-TUBA4 levels was observed in NTM cells (Fig. 5B). In GTM cells, higher levels of Ac-TUBA4 were found in those cultured on 900-kPa plates compared to 60-kPa CellSoft BioFlex plates, but not in those cultured on plastic plates (Fig. 5B). Overall, these results do not support a direct effect of substrate stiffness on tubulin acetylation.

Tubulin Acetylation Does Not Affect Cell Contractility in TM Cells

Recent studies in other cell types have suggested a role of tubulin acetylation in regulating cell contractility.[12,32] Given the relevance of TM cell contractility on AH outflow,[9,33,34] we aimed to determine if this was also true for TM cells. To test this, we performed a collagen-based gel cell contractility assay in TM cells with knocked-down expression of ATAT1

Investigative Ophthalmology & Visual Science

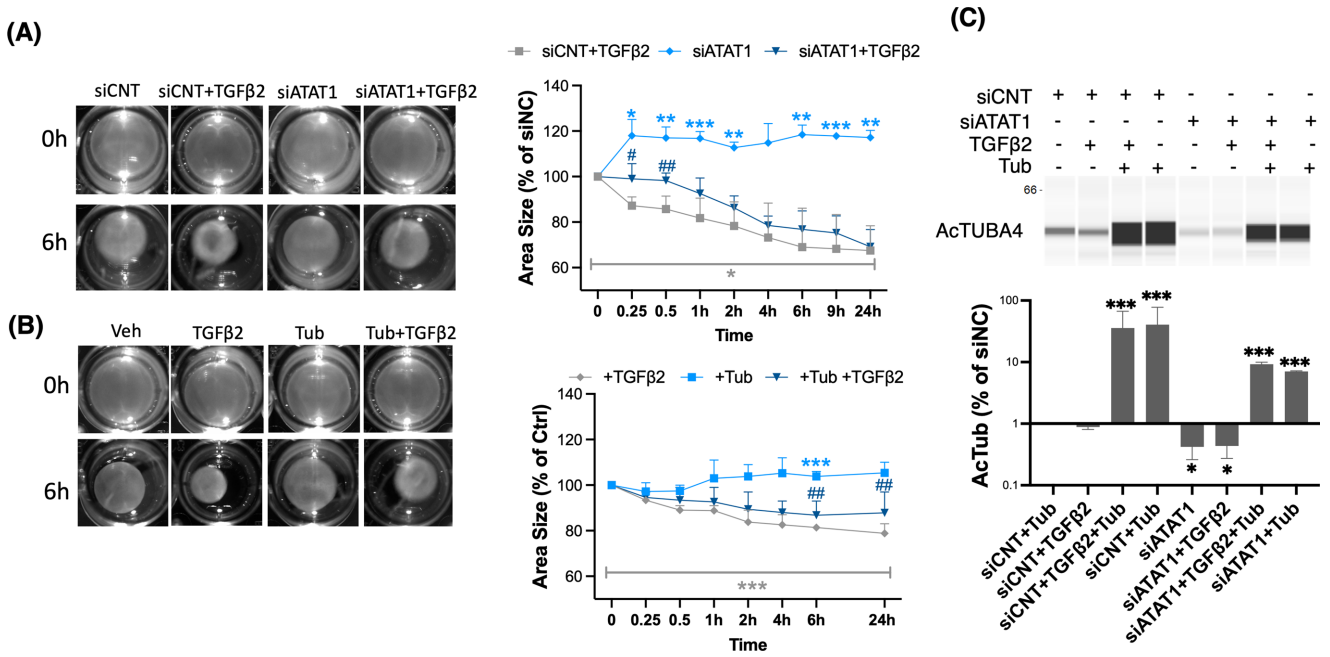

Figure 6. Effect of tubulin acetylation on TM cell contractility. (**A**) Primary TM cells were transfected with siATAT1 or siCNT. At day 1 post-transfection, cells were embedded in the collagen gel and incubated for 24 hours, followed by another 24 hours of incubation with TGFβ2 (10 ng/mL) or vehicle control in fresh media. A representative picture of gel contractility is shown. The area of the gel was measured. Changes in gel size over time were calculated and compared to siCNT control ($n = 3$; $^{*,\#}P < 0.05$, $^{**,\#\#}P < 0.01$, $^{***}P < 0.001$, *t*-test). (**B**) Primary TM cells embedded in collagen gel were pretreated with either 1.25 µM of tubacin or DMSO for 6 hours and then incubated for 24 hours with TGFβ2 (10 ng/mL) or vehicle control in fresh media in the presence of tubacin or DMSO. Changes in the gel size over time were calculated and compared to vehicle control. (**C**) Ac-TUBA4 levels evaluated by the Jess Simple WB system and quantified using the automated built-in total protein normalization ($n = 3$; $^{*}P < 0.05$, $^{***}P < 0.001$, ANOVA with multiple comparisons).

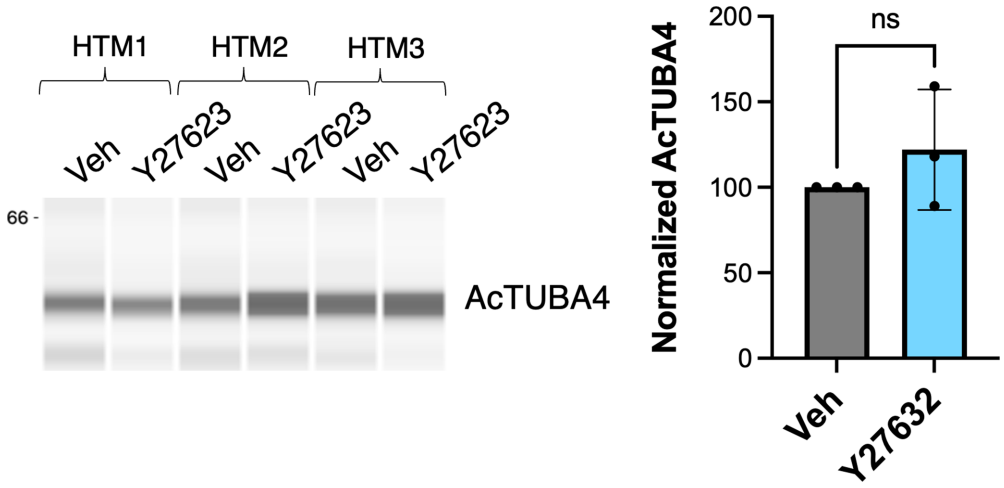

Figure 7. Effect of Rho kinase inhibitor on tubulin acetylation. TM primary cultures were treated with the Rho kinase inhibitor Y27632 (10 µM) for 24 hours. Ac-TUBA4 levels were evaluated by the Jess Simple WB system and quantified using the automated built-in total protein normalization ($n = 3$; ns, not significant, *t*-test).

(siATAT1). Cells treated with TGFβ2 (10 ng/mL) served as positive control. The area of the non-released gel lattice was measured, and the change in gel size at the indicated times after release was calculated (Fig. 6A). To evaluate the efficacy of the treatments, we simultaneously conducted the experiments in cells cultured under the same conditions without gel.

Neither siATAT1 nor TGFβ2 treatment affected the size of the unreleased gel (Supplementary Fig. S2A). As expected, treatment with TGFβ2 promoted cell contractility, showing a reduction in gel area size over time (Fig. 6A). Confirming previous studies, silencing ATAT1 expression resulted in relaxation of the collagen gel compared to siCNT-transfected cells. Furthermore, ATAT1 knockdown also inhibited TGFβ2-induced contractility, particularly during the first hour after release (Fig. 6A). Western blot analysis confirmed lower Ac-TUBA4 levels in siATAT1 cultures (Fig. 6C).

Investigative Ophthalmology & Visual Science

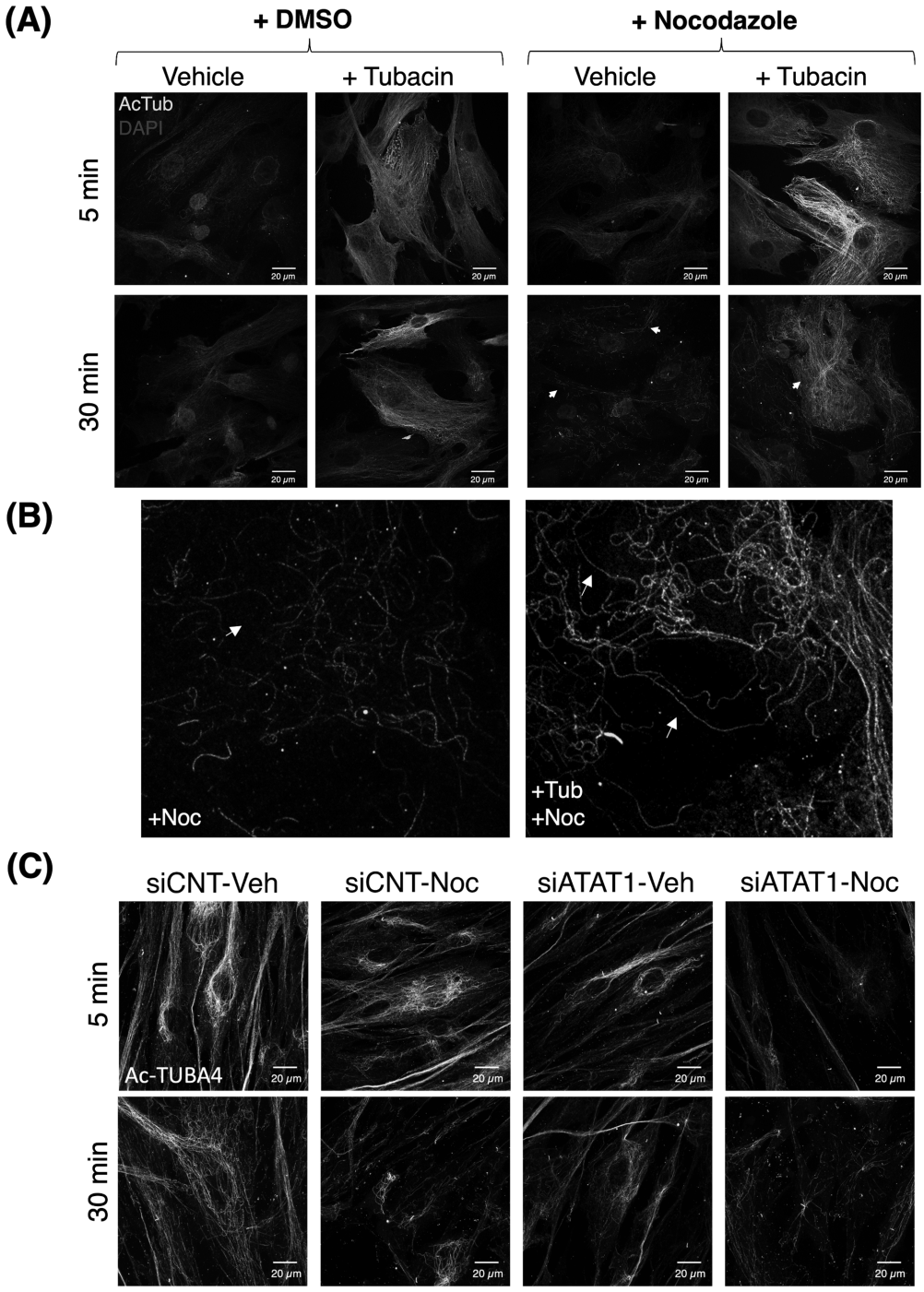

Figure 8. Tubulin acetylation protects against nocodazole-induced microtubule depolymerization. (**A**) Immunocytochemical evaluation of Ac-TUBA4 in TM cells treated for 24 hours with tubacin (1.25 µM) and exposed to the tubulin depolymerizing agent nocodazole (1 µM) during the indicated time. (**B**) Higher magnification pictures of acetylated-labeled microtubules (*arrows*). (**C**) Immunocytochemical evaluation of Ac-TUBA4 in siATAT1- or siCNT-transfected TM cells exposed to nocodazole (1 µM) or vehicle for the indicated times.

Next, we evaluated the effect of tubacin, a potent HDAC6 inhibitor that suppresses tubulin deacetylation, leading to a significant increase in acetylated tubulin content (Fig. 6C, Supplementary Fig. S3). We tested the effect of tubacin treatment alone (Fig. 6B) and its potential to rescue the siATAT1 phenotype (Supplementary Fig. S2B). No significant effect of tubacin on gel size was observed in either the unreleased or released gel compared to the vehicle control (Supplementary Fig. S2A). Unexpectedly, tubacin treatment led to a decrease in TGFβ2-induced cell contractility, which became statistically significant 6 hours post-release (Fig. 6B). Moreover, tubacin treatment did not reverse the cell relaxation observed in siATAT1-transfected cultures (Supplementary Fig. S2B), despite the much higher acetylated tubulin content (Fig. 6C).

Investigative Ophthalmology & Visual Science

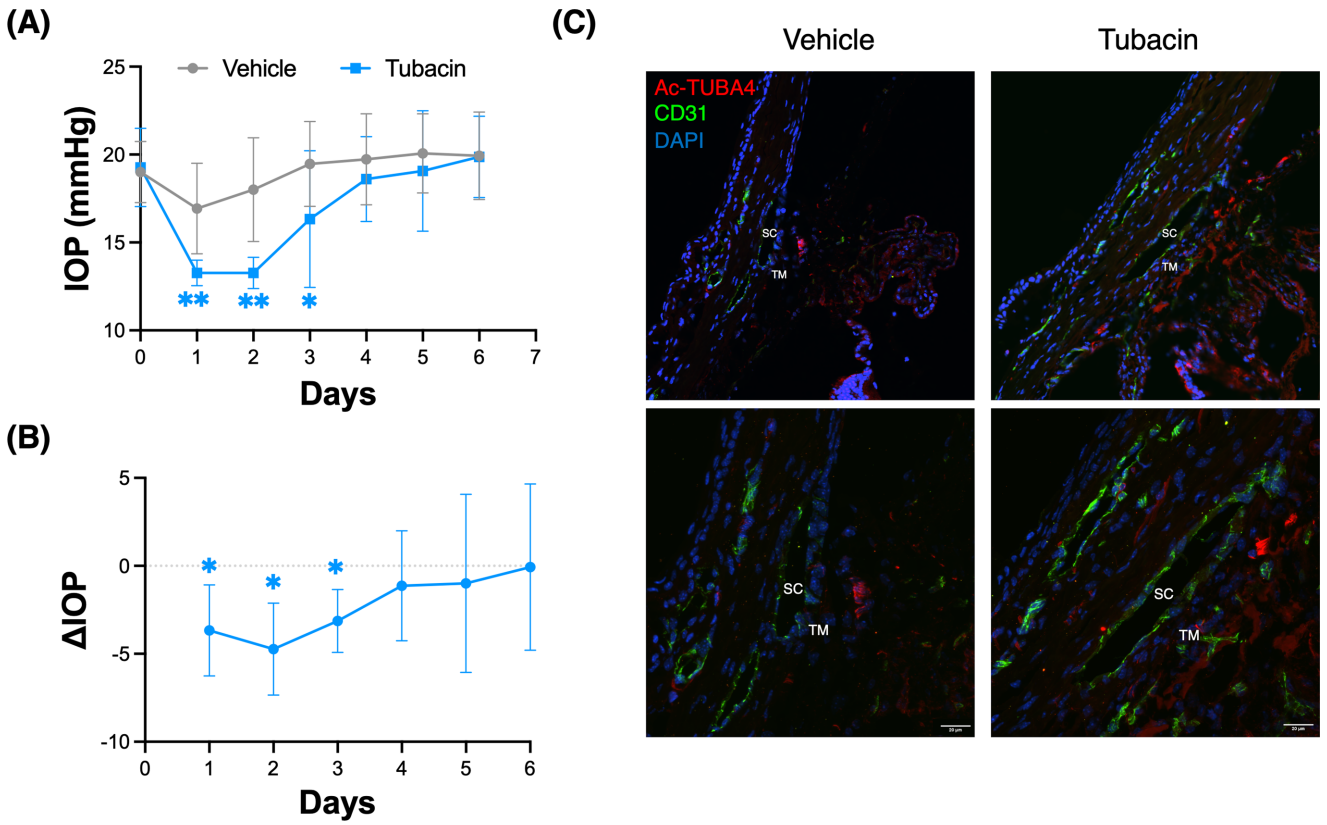

Figure 9. Tubacin treatment lowers IOP in mice. (**A**) Diurnal IOP measurements over time in C57BL/6J mice intracamerally injected with tubacin (2 µL of 10-µM stock solution) or vehicle ($n = 5$; $^{*}P < 0.05$, $^{**}P < 0.01$, *t*-test). (**B**) Delta IOP compared to the contralateral vehicle-treated eye ($n = 5$; $^{*}P < 0.05$, paired *t*-test). (**C**) Representative immunofluorescence in frozen sections stained for Ac-TUBA4. CD31 staining was used to better visualize SC, and DAPI was used to stain the nuclei.

We also explored whether Rho kinase inhibitor could alter tubulin acetylation levels. As shown in Figure 7, no significant changes in Ac-TUBA4 levels were detected in TM cells treated with the Rho kinase inhibitor Y27623. Together, these findings support a role for ATAT1, but not tubulin acetylation, in regulating cell contractility in TM cells.

Tubulin Acetylation Protects Against Microtubule Breakage in TM Cells

Acetylation of tubulin at K40 has been proposed to provide stability and protect against microtubule breakage. To test this hypothesis, we determined whether the increased levels of tubulin acetylation induced by tubacin treatment could protect against microtubule depolymerization induced by nocodazole, a known microtubule-depolymerizing agent. TM cells were treated with tubacin (1.25 µM) for 24 hours, followed by incubation with nocodazole or DMSO vehicle control. Cells were then fixed at the indicated times, and Ac-TUBA4 levels were analyzed by immunofluorescence. As expected, nocodazole treatment led to extensive microtubule depolymerization. However, cells pretreated with tubacin exhibited increased qualitative levels of acetylated microtubules, even after nocodazole exposure, compared to vehicle-treated controls (Fig. 8A). Moreover, higher magnification images revealed that microtubules in tubacin-treated cells were less sinuous and longer and exhibited fewer fractures (Fig. 8B).

To further confirm a role of tubulin acetylation in microtubule stabilization, we conducted similar experiments in TM cells transfected with siATAT1. Knockdown of ATAT1 reduced Ac-TUBA4 levels (Fig. 8C). Furthermore, nocodazole treatment resulted in a more rapid and pronounced depolymerization effect in siATAT1 compared to siCNT transfected cells, with almost no visible intact acetylated microtubule observed at 30 minutes post-treatment.

Intracameral Injection of Tubacin Lowers IOP

Next, we investigated the effect of tubulin acetylation on IOP. To do this, we administered an intracameral injection of tubacin (10 µM) into the anterior chamber of C57BL/6J mice, with the contralateral eye receiving a DMSO vehicle control injection. Following this initial injection, either DMSO or tubacin (10 µM) was applied topically as eye drops daily for 6 days as a supplementary treatment. Diurnal IOP measurements were recorded (Fig. 9A), and variations in IOP in the tubacin-treated eyes were compared to their fellow eyes at each time point (Fig. 9B). A significant decrease in IOP was observed in the tubacin-injected eyes on day 1 (-3.66 ± 2.5 mm Hg, $P = 0.009$, $n = 5$), day 2 (-4.73 ± 2.6 mm Hg, $P = 0.0013$, $n = 5$), and day 3 (-3.13 ± 1.7 mm Hg, $P = 0.05$, $n = 5$) post-injection compared to their respective fellow eyes, gradually returning to the baseline levels. This indicates that the IOP-lowering effect of tubacin is primarily attributable to the intracameral injection rather than the topical application. This finding aligns with unpublished evidence from our

lab showing no significant IOP-lowering effect from topical application of tubacin alone. Higher Ac-TUBA4 levels in the TM and ciliary body in the tubacin-injected eyes were confirmed by immunofluorescence (Fig. 9C).

Discussion

This study provides novel insights into the mechanobiology of TM cells by demonstrating that mechanical stretch induces acetylation of α-tubulin at lysine 40. Our findings reveal that mechanical forces can modulate MT dynamics in TM cells through the regulation of tubulin acetylation, a post-translational modification known to enhance MT stability. We have also shown that elevated levels of Ac-TUBA4 are present in GTM cells and that enhancing tubulin acetylation in vivo leads to a reduction in IOP in mice. These results suggest that tubulin acetylation is a critical adaptive response of TM cells to mechanical stress and may represent a potential therapeutic target for glaucoma.

The regulation of tubulin acetylation in TM cells appears to be mediated by the coordinated action of the acetyltransferase ATAT1 and the deacetylase HDAC6. Interestingly, SIRT2, another deacetylase implicated in tubulin acetylation in other cell types,[17] did not significantly affect Ac-TUBA4 levels when knocked down, suggesting a minimal role in TM cells. Under CMS conditions, we observed a significant reduction in HDAC6 protein levels without changes in ATAT1 mRNA levels. Although we cannot completely exclude a role for ATAT1 in this process due to the lack of availability of commercial antibodies to detect ATAT1, our results suggest that mechanical stretch promotes tubulin acetylation primarily by downregulating HDAC6, thereby decreasing tubulin deacetylation rates. This is consistent with previous reports in a lung adenocarcinoma cell line.[35]

Immunofluorescence analysis of human ocular tissues showed increased Ac-TUBA4 staining in the TM region of glaucomatous eyes. Elevated levels of Ac-TUBA4 were also observed in GTM compared to NTM primary cultures by western blot, suggesting a possible link between tubulin acetylation and glaucomatous pathology. The elevated tubulin acetylation in GTM cells may reflect a compensatory mechanism to counteract increased mechanical stress due to elevated IOP or changes in extracellular matrix stiffness commonly associated with glaucoma. In this regard, extracellular matrix stiffness has been reported to induce tubulin acetylation in astrocytes[12] and fibroblasts.[36] Contrary to our initial hypothesis, substrate stiffness did not directly or proportionally influence tubulin acetylation levels in TM cells. No significant effect of substrate stiffness was observed in NTM cells. Although Ac-TUBA4 levels increased in GTM cells at 900 kPa compared to 60 kPa, this effect was not observed at 1 GPa. These findings suggest that (1) mechanical stretch, rather than substrate stiffness alone, serves as the primary regulator of tubulin acetylation in these cells; and (2) highlight the importance of dynamic mechanical forces, as opposed to static mechanical properties, in modulating MT dynamics in the TM. That might not be the case, however, in glaucomatous tissue, based on the lower induction of Ac-TUBA4 observed with CMS in GTM cells.

Microtubules enriched in acetylated tubulin increase cytoskeletal stiffness and viscoelastic resistance in cardiomyocytes and muscle cells, which in turn slows the rates of contraction and relaxation.[37] Although we did not measure cortical stiffness, we explored the functional consequences of modulating tubulin acetylation on TM cell contractility, a critical factor influencing AH outflow resistance. ATAT1 knockdown led to reduced cell contractility and inhibited TGFβ2-induced contractility in collagen gel assays, as also reported in fibroblasts[12,38]; however, increasing tubulin acetylation using tubacin did not enhance contractility in TM cells. In fact, tubacin treatment decreased TGFβ2-induced contractility. Although differences between genetic and pharmacological interventions could contribute to the contrasting results, tubacin treatment did not reverse the relaxation observed in ATAT1-silenced cells, despite significantly increasing Ac-TUBA4 levels. Additionally, inhibition of Rho kinase did not affect Ac-TUBA4 levels, suggesting that tubulin acetylation does not directly influence the contractile machinery of TM cells. These findings indicate that ATAT1 may regulate cell contractility through mechanisms independent of tubulin acetylation, possibly involving other substrates or pathways.

Our results support the notion that tubulin acetylation enhances MT stability and protects against microtubule breakage in TM cells. Pretreatment with tubacin conferred resistance to nocodazole-induced MT depolymerization, as evidenced by the preservation of longer and less fragmented microtubules. Conversely, ATAT1 knockdown accelerated MT depolymerization upon nocodazole exposure, as also reported in Xu et al.[23]

Tubulin acetylation at K40 on α-tubulin is a hallmark of long-lived MTs.[15,39] Although it remains controversial whether tubulin acetylation is a causative factor or merely correlates with microtubule stabilization, emerging evidence suggests that acetylation actively contributes to enhancing MT flexibility and mechanical resilience.[17] Unlike other tubulin post-translational modifications such as polyglutamylation, polyglycylation, and detyrosination—which occur on the outer surface of MTs—acetylation uniquely takes place on the inner, luminal surface.[40,41] Structural studies, including cryo-electron microscopy analyses, have revealed that acetylation at K40 alters the conformation of an unstructured loop in α-tubulin.[15,24] This alteration reduces lateral interactions between protofilaments by weakening inter-protofilament contacts, promoting protofilament sliding, and increasing MT flexibility. Enhanced flexibility allows MTs to withstand repetitive mechanical stresses without accumulating damage, effectively protecting them from mechanical aging. Thus, acetylation enhances the mechanical properties of MTs contributing to their stability and longevity within the cellular environment.[12,15,23,24,39] How acetylation contributes to stability and protects against depolymerization is still unknown. It is possible that acetylation affects other post-translational modifications and/or interactions with MT-associated proteins.[42]

Long-lived MTs are frequently highly buckled due to the compressive loads generated by MT-based molecular motors and actomyosin contractility.[32] Therefore, increased flexibility imparted by acetylation is crucial for their persistence and function.[14,19] Notably, the localization of Ac-TUBA4 shifted from a predominantly perinuclear region in non-stretched cells to a more extensive cytoplasmic distribution in stretched cells. This suggests that mechanical stretch not only enhances tubulin acetylation but also alters the spatial organization of acetylated MTs, potentially affecting cellular functions such as intracellular transport and signal transduction.

Importantly, we demonstrated that increasing tubulin acetylation in vivo via intracameral injection of tubacin leads to a significant reduction in IOP in mice. The IOP-

Investigative Ophthalmology & Visual Science

lowering effect was observed within the first 3 days post-injection without any signs of ocular inflammation or structural abnormalities. The IOP-lowering effect of tubacin is in contrast to the IOP elevation reported by Bermudez et al.,[43] who perfused bovine eyes with the HDAC inhibitor thailandepsin A (TDP-A). Note that TDP-A and tubacin target structurally and functionally different HDACs with distinct subcellular expression patterns. Class I HDACs are constitutively nuclear proteins and participate in epigenetic modification of histones. In contrast, tubacin selectively targets HDAC6, a Class IIb HDAC6 located in the cytosol.[44] Our findings suggest, first, that enhancing tubulin acetylation in TM cells may improve aqueous humor outflow by stabilizing the MT network, thereby reducing outflow resistance, and, second, that the elevated tubulin acetylation observed in glaucomatous TM cells and tissue may reflect a compensatory mechanism to counteract increased mechanical stress due to elevated IOP, rather than being the cause of elevated IOP. Targeting tubulin acetylation and MT stability might represent a promising therapeutic strategy.

Conclusions

Our study highlights the critical role of tubulin acetylation in TM cell response to mechanical stress and its potential impact on IOP regulation. Mechanical stretch induces tubulin acetylation in TM cells by downregulating HDAC6, leading to enhanced MT stability. Elevated tubulin acetylation in glaucomatous TM cells suggests a compensatory mechanism to counteract increased mechanical load. Although tubulin acetylation does not appear to modulate TM cell contractility directly, it plays a protective role against MT destabilization. The IOP-lowering effect of tubacin in vivo underscores the therapeutic potential of modulating tubulin acetylation in glaucoma management. Future studies should explore the molecular mechanisms underlying the influence of ATAT1 on cell contractility and investigate the long-term effects of targeting tubulin acetylation in ocular physiology and pathology.

Acknowledgments

Supported by grants from the National Eye Institute, National Institutes of Health (EY026885, EY033600, and P30EY005722 to PBL; EY019643, EY032590, and P30EY010572 to KEK); an unrestricted grant from Research to Prevent Blindness (PBL); and a grant from the Taiwan National Science and Technology Council (113-2314-B-002-074 to C-CS).

Disclosure: **C.-C. Su**, None; **V. Desikan**, None; **K. Betsch**, None; **M.S. Shim**, None; **K.E. Keller**, None; **P.B. Liton**, None

References

1. Acott TS, Kelley MJ, Keller KE, et al. Intraocular pressure homeostasis: maintaining balance in a high-pressure environment. *J Ocul Pharmacol Ther*. 2014;30:94–101.
2. Sherwood JM, Stamer WD, Overby DR. A model of the oscillatory mechanical forces in the conventional outflow pathway. *J R Soc Interface*. 2019;16:20180652.
3. Krishnan R, Park CY, Lin YC, et al. Reinforcement versus fluidization in cytoskeletal mechanoresponsiveness. *PLoS One*. 2009;4:e5486.
4. Vittal V, Rose A, Gregory KE, Kelley MJ, Acott TS. Changes in gene expression by trabecular meshwork cells in response to mechanical stretching. *Invest Ophthalmol Vis Sci*. 2005;46:2857–2868.
5. Trepat X, Deng L, An SS, et al. Universal physical responses to stretch in the living cell. *Nature*. 2007;447:592–595.
6. Hamant O, Inoue D, Bouchez D, Dumais J, Mjolsness E. Are microtubules tension sensors? *Nat Commun*. 2019;10:2360.
7. Tumminia SJ, Mitton KP, Arora J, Zelenka P, Epstein DL, Russell P. Mechanical stretch alters the actin cytoskeletal network and signal transduction in human trabecular meshwork cells. *Invest Ophthalmol Vis Sci*. 1998;39:1361–1371.
8. Luna C, Li G, Liton PB, Epstein DL, Gonzalez P. Alterations in gene expression induced by cyclic mechanical stress in trabecular meshwork cells. *Mol Vis*. 2009;15:534–544.
9. Rao PV, Deng PF, Kumar J, Epstein DL. Modulation of aqueous humor outflow facility by the Rho kinase-specific inhibitor Y-27632. *Invest Ophthalmol Vis Sci*. 2001;42:1029–1037.
10. Ethier CR, Read AT, Chan D. Biomechanics of Schlemm's canal endothelial cells: influence on F-actin architecture. *Biophys J*. 2004;87:2828–2837.
11. Janke C, Magiera MM. The tubulin code and its role in controlling microtubule properties and functions. *Nat Rev Mol Cell Biol*. 2020;21:307–326.
12. Seetharaman S, Vianay B, Roca V, et al. Microtubules tune mechanosensitive cell responses. *Nat Mater*. 2022;21:366–377.
13. Palazzo A, Ackerman B, Gundersen GG. Cell biology: Tubulin acetylation and cell motility. *Nature*. 2003;421:230.
14. Carmona B, Marinho HS, Matos CL, Nolasco S, Soares H. Tubulin post-translational modifications: the elusive roles of acetylation. *Biology (Basel)*. 2023;12:561.
15. Eshun-Wilson L, Zhang R, Portran D, et al. Effects of alpha-tubulin acetylation on microtubule structure and stability. *Proc Natl Acad Sci USA*. 2019;116:10366–10371.
16. Sadoul K, Khochbin S. The growing landscape of tubulin acetylation: lysine 40 and many more. *Biochem J*. 2016;473:1859–1868.
17. Li L, Yang XJ. Tubulin acetylation: responsible enzymes, biological functions and human diseases. *Cell Mol Life Sci*. 2015;72:4237–4255.
18. Perdiz D, Mackeh R, Pous C, Baillet A. The ins and outs of tubulin acetylation: more than just a post-translational modification? *Cell Signal*. 2011;23:763–771.
19. Nekooki-Machida Y, Hagiwara H. Role of tubulin acetylation in cellular functions and diseases. *Med Mol Morphol*. 2020;53:191–197.
20. Shida T, Cueva JG, Xu Z, Goodman MB, Nachury MV. The major α-tubulin K40 acetyltransferase αTAT1 promotes rapid ciliogenesis and efficient mechanosensation. *Proc Natl Acad Sci USA*. 2010;107:21517–21522.
21. Kalebic N, Sorrentino S, Perlas E, Bolasco G, Martinez C, Heppenstall PA. αTAT1 is the major α-tubulin acetyltransferase in mice. *Nat Commun*. 2013;4:1962.
22. Friedmann DR, Aguilar A, Fan J, Nachury MV, Marmorstein R. Structure of the α-tubulin acetyltransferase, αTAT1, and implications for tubulin-specific acetylation. *Proc Natl Acad Sci USA*. 2012;109:19655–19660.
23. Xu Z, Schaedel L, Portran D, et al. Microtubules acquire resistance from mechanical breakage through intralumenal acetylation. *Science*. 2017;356:328–332.
24. Portran D, Schaedel L, Xu Z, Thery M, Nachury MV. Tubulin acetylation protects long-lived microtubules against mechanical ageing. *Nat Cell Biol*. 2017;19:391–398.
25. Porter KM, Jeyabalan N, Liton PB. MTOR-independent induction of autophagy in trabecular meshwork cells subjected to biaxial stretch. *Biochim Biophys Acta*. 2014;1843:1054–1062.

26. Keller KE, Bhattacharya SK, Borras T, et al. Consensus recommendations for trabecular meshwork cell isolation, characterization and culture. *Exp Eye Res*. 2018;171:164–173.
27. Shim MS, Nettesheim A, Dixon A, Liton PB. Primary cilia and the reciprocal activation of AKT and SMAD2/3 regulate stretch-induced autophagy in trabecular meshwork cells. *Proc Natl Acad Sci USA*. 2021;118:e2021942118.
28. Wang K, Li G, Read AT, et al. The relationship between outflow resistance and trabecular meshwork stiffness in mice. *Sci Rep*. 2018;8:5848.
29. Wang K, Read AT, Sulchek T, Ethier CR. Trabecular meshwork stiffness in glaucoma. *Exp Eye Res*. 2017;158:3–12.
30. Camras LJ, Stamer WD, Epstein D, Gonzalez P, Yuan F. Circumferential tensile stiffness of glaucomatous trabecular meshwork. *Invest Ophthalmol Vis Sci*. 2014;55:814–823.
31. Last JA, Pan T, Ding Y, et al. Elastic modulus determination of normal and glaucomatous human trabecular meshwork. *Invest Ophthalmol Vis Sci*. 2011;52:2147–2152.
32. Fernandez-Barrera J, Alonso MA. Coordination of microtubule acetylation and the actin cytoskeleton by formins. *Cell Mol Life Sci*. 2018;75:3181–3191.
33. Tian B, Gabelt BT, Geiger B, Kaufman PL. The role of the actomyosin system in regulating trabecular fluid outflow. *Exp Eye Res*. 2009;88:713–717.
34. Tian B, Kaufman PL, Volberg T, Gabelt BT, Geiger B. H-7 disrupts the actin cytoskeleton and increases outflow facility. *Arch Ophthalmol*. 1998;116:633–643.
35. Geiger RC, Kaufman CD, Lam AP, Budinger GR, Dean DA. Tubulin acetylation and histone deacetylase 6 activity in the lung under cyclic load. *Am J Respir Cell Mol Biol*. 2009;40:76–82.
36. Wen D, Gao Y, Liu Y, et al. Matrix stiffness-induced α-tubulin acetylation is required for skin fibrosis formation through activation of Yes-associated protein. *MedComm (2020)*. 2023;4:e319.
37. Coleman AK, Joca HC, Shi G, Lederer WJ, Ward CW. Tubulin acetylation increases cytoskeletal stiffness to regulate mechanotransduction in striated muscle. *J Gen Physiol*. 2021;153:e202012743.
38. You E, Ko P, Jeong J, et al. Dynein-mediated nuclear translocation of Yes-associated protein through microtubule acetylation controls fibroblast activation. *Cell Mol Life Sci*. 2020;77:4143–4161.
39. Szyk A, Deaconescu AM, Spector J, et al. Molecular basis for age-dependent microtubule acetylation by tubulin acetyltransferase. *Cell*. 2014;157:1405–1415.
40. Coombes C, Yamamoto A, McClellan M, et al. Mechanism of microtubule lumen entry for the α-tubulin acetyltransferase enzyme αTAT1. *Proc Natl Acad Sci USA*. 2016;113:E7176–E7184.
41. Al-Bassam J, Corbett KD. α-Tubulin acetylation from the inside out. *Proc Natl Acad Sci USA*. 2012;109:19515–19516.
42. Asthana J, Kapoor S, Mohan R, Panda D. Inhibition of HDAC6 deacetylase activity increases its binding with microtubules and suppresses microtubule dynamic instability in MCF-7 cells. *J Biol Chem*. 2013;288:22516–22526.
43. Bermudez JY, Webber HC, Patel GC, et al. HDAC inhibitor-mediated epigenetic regulation of glaucoma-associated TGFβ2 in the trabecular meshwork. *Invest Ophthalmol Vis Sci*. 2016;57:3698–3707.
44. Morris MJ, Monteggia LM. Unique functional roles for class I and class II histone deacetylases in central nervous system development and function. *Int J Dev Neurosci*. 2013;31:370–381.

Investigative Ophthalmology & Visual Science